Enhanced denitrification in groundwater and sediments from a nitrate-contaminated aquifer after addition of pyrite

Clara Torrentó [(1)], Jordi Urmeneta [(2)], Neus Otero [(3)], Albert Soler [(3)], Marc Viñas [(4)] and Jordi Cama [(1)]

(1) Grup de Hidrogeoquímica, Institut de Diagnosi Ambiental i Estudis de l'Aigua IDAEA, CSIC, C/Jordi Girona, 18-26, 08034 Barcelona, Spain. clara.torrento@idaea.csic.es, jordi.cama@idaea.csic.es

(2) Departament de Microbiologia i Institut de Recerca de la Biodiversitat (IRBio), Universitat de Barcelona (UB), Av. Diagonal 645, 08028 Barcelona, Spain. jurmeneta@ub.edu

(3) Grup de Mineralogia Aplicada i Medi Ambient, Departament de Cristal·lografia, Mineralogia i Dipòsits Minerals, Facultat de Geologia, Universitat de Barcelona (UB), Martí i Franquès s/n, 08028 Barcelona, Spain. notero@ub.edu, albertsolergil@ub.edu

(4) Centre Tecnològic GIRO, Rambla Pompeu Fabra 1, 08100 Mollet del Vallès, Barcelona, Spain. marc.vinas@giroct.irta.cat

(*) Corresponding author: Clara Torrentó e-mail: clara.torrento@idaea.csic.es Fax: +34 93 411 00 12.

Abstract

Using chemical, isotopic and microbiologic techniques we tested in laboratory experiments the extent to which the addition of pyrite to groundwater and sediments from a nitrate-contaminated aquifer could stimulate denitrification by indigenous bacteria. In addition to this biostimulated approach, a combined biostimulated and bioaugmented treatment was also evaluated by inoculating the well-known autotrophic denitrifying bacterium *Thiobacillus denitrificans*. Results showed that the addition of pyrite enhanced nitrate removal and that denitrifying bacteria existing in the aquifer material were able to reduce nitrate using pyrite as the electron donor, obviating the need for the inoculation of *T. denitrificans*. The results of the *16S rRNA* and *nosZ* gene-based DGGE and the quantitative PCR (qPCR) showed that the addition of pyrite led to an increase in the proportion of denitrifying bacteria and that bacterial populations closely related to the *Xanthomonadaceae* might probably be the autotrophic denitrifiers that used pyrite as the electron donor. Not only autotrophic but also heterotrophic denitrifying bacteria were stimulated through pyrite addition and both populations probably contributed to nitrate removal. Isotopic analyses ($\delta^{15}N$ and $\delta^{18}O_{NO3}$) were used to monitor enhanced denitrification and the N and O isotopic enrichment factors (-26.3±1.8‰ and -20.4±1.3‰, respectively) allowed to calculate the degree of natural nitrate attenuation in the aquifer. Furthermore, flow-through experiments amended with pyrite confirmed the long-term efficiency of the process under the study conditions. Further research under field conditions is needed to determine whether stimulation of denitrification by pyrite addition constitutes a feasible bioremediation strategy for nitrate-contaminated aquifers.

Keywords: bioremediation, autotrophic denitrification, pyrite, DGGE, qPCR, nitrate isotopes

1. INTRODUCTION

Nitrate is one of the most common contaminants in groundwater. A high nitrate concentration in drinking water poses a considerable health risk (Ward et al., 2005). Moreover, a high nitrate level in surface waters constitutes a serious threat to aquatic ecosystems owing to the increase of algal growth, which contributes to eutrophication.

Denitrification is the most significant process removing nitrate in natural environments. Denitrification occurs naturally when certain bacteria use nitrate as the terminal electron acceptor in their respiratory processes in the absence of oxygen (Zumft, 1997). Most denitrifying bacteria are heterotrophic bacteria, which utilize simple organic carbon compounds as the electron donor. Nevertheless, other denitrifying bacteria are autotrophic and are able to couple the reduction of nitrate with the oxidation of inorganic compounds. Given the ubiquity of denitrifying bacteria in nature, denitrification takes place naturally in aquifers, soils and seawater when the necessary environmental conditions arise simultaneously.

The Osona area (NE Spain) is affected by widespread groundwater nitrate contamination resulting from the excessive application of pig manure as fertilizer. Natural attenuation of nitrate pollution has been reported in some zones of this area (Otero et al., 2009; Vitòria et al., 2008). The occurrence of these denitrification processes is related to pyrite oxidation, as Otero et al. (2009) demonstrated by coupling nitrate and sulfate isotopic data. Other field studies have also suggested that pyrite oxidation regulates denitrification in aquifers even in the presence of organic carbon (e.g. Aravena and Robertson, 1998; Pauwels et al., 2000; Postma et al., 1991). This pyrite-driven denitrification reaction has been demonstrated at the laboratory scale (Jorgensen et al., 2009; Torrentó et al., 2010).

Denitrification in natural systems proceeds very slowly and is not very effective in lowering nitrate concentrations in aquifers. This is why several technologies have been developed for removing nitrate (Della Rocca et al., 2007). A conceivable bioremediation strategy is biostimulation of the indigenous denitrifying bacteria by addition of suitable electron donors (Soares, 2000). This strategy requires the existence of an indigenous microbial community able to reduce nitrate using the added electron donor. Where the appropriate denitrifying bacteria are not present, bioaugmentation can accelerate the removal of nitrate by introducing specialized bacteria (Vogel, 1996).

Torrentó et al. (2010) showed that biostimulation by addition of pyrite is a feasible remediation strategy for nitrate-contaminated aquifers, although care should be taken to avoid significant release of trace metals and sulfate as a result of pyrite oxidation (Larsen and Postma, 1997; Smolders et al., 2006; 2010). Before applying this bioremediation strategy in the field, it is necessary to evaluate whether indigenous microorganisms with potential to reduce nitrate using pyrite as the electron donor are present in the Osona aquifer material.

This study is aimed at evaluating a potential denitrification enhancement by addition of pyrite. Pyrite-amended batch and flow-through experiments were performed using saturated material and groundwater from the Osona aquifer. We examined the persistence of this biostimulation strategy over a relatively long time frame (6 months). Also, the feasibility of a combined biostimulated and bioaugmented treatment was evaluated. This was accomplished by inoculating the experiments with the bacterium *Thiobacillus denitrificans*, which is able to reduce nitrate using pyrite as the electron donor (Torrentó et al., 2010). Furthermore, the diversity of the indigenous microbial community and its response to the different treatments were determined in order to gain insight into the progress of natural attenuation and to further improve bioremediation processes. Finally, the N and O isotopic enrichment factors were calculated to

69 better approximate the degree of natural denitrification in the Osona aquifer and to assess the
70 efficacy of the induced attenuation.

71 ## 2. EXPERIMENTAL METHODOLOGY

72 ### 2.1. Study site

73 The Osona region is an area that is classified as vulnerable to nitrate pollution from
74 agricultural sources following the European Nitrate Directive (91/676/EEC). Considerable
75 amounts of pig manure are produced as a result of intensive farming and most of this manure is
76 used as organic fertilizer, leading to widespread groundwater nitrate contamination.
77 Hydrogeologically, the system is made up of a series of confined aquifers located in carbonate
78 and carbonate-sandstone layers, whose porosity is mainly related to the fracture network (Menció
79 et al., 2010; Otero et al., 2009). These formations are interbedded in confining marl layers that
80 contain disseminated pyrite (Menció et al., 2010).

81 ### 2.2. Material and characterization

82 A core hole (Roda de Ter, Osona region) was drilled to a depth of 12 m, about 3 m below
83 the groundwater table, and material was sampled with a core barrel. After removing the core
84 from the barrel, a core fragment was immediately preserved at 4°C in an autoclaved glass flask
85 with a CO_2 atmosphere generated by a BBL® disposable gas generator envelope. Immediately
86 before the start of the experiments, the core fragment was crushed to centimeter-sized fragments
87 under sterile and anaerobic conditions.

88 Powder X-ray diffraction (XRD) of the core sample was performed using a Bruker D5005
89 diffractometer with Cu Kα radiation over a 2θ range from 0 to 60 degrees, with a scan speed of
90 0.025°/18 s. Rietveld analyses revealed that the sample was mainly composed of calcite (27.2

91 wt%), muscovite (26.2 wt%) and quartz (23.1 wt%) with small amounts of albite (10.3 wt%),
92 dolomite (7.7 wt%), sudoite (4.9 wt%) and pyrite (0.6 wt%).

93 Groundwater samples were collected from a well close to the drilling site in sterilized glass
94 bottles filled completely to avoid air in the bottle headspace and stored at 4°C until used. Aseptic
95 sampling techniques and sterile sample containers were used to prevent contamination of
96 groundwater with non-native bacteria. The pH of the water was 6.84 and the water was classified
97 as bicarbonate-calcium type in accordance with the lithology of the aquifer. Groundwater had an
98 elevated nitrate concentration (1.7 mM) and nitrite was below the detection limit (0.2 μM). When
99 sterile material was needed (Table 1), core fragments and groundwater were sterilized by
100 autoclaving at 121°C for 15 min.

101 Natural pyrite crystals were obtained from sedimentary deposits in Navajún (Logroño, NE
102 Spain). Fragments were crushed and sieved to obtain a size particle that ranged from 50 to 100
103 μm. The X-ray patterns confirmed the samples to be pyrite and showed no evidence of the
104 presence of any other mineral phase. The chemical composition of pyrite was determined by
105 electron microprobe analysis (EMPA) using a Cameca SX-50. The pyrite atomic composition (at.
106 %) was 66.46±0.37 of S and 33.34±0.21 of Fe based on 20 points. Impurities of Ni were detected
107 (0.07±0.05 at. %) and Co, Cu, Zn, As and Pb were below detection limits (0.02, 0.03, 0.03, 0.02 and
108 0.19 at. %, respectively). Before the start of the experiments, powdered pyrite was sterilized by
109 autoclaving at 121°C for 15 min.

110 *Thiobacillus denitrificans* (strain 12475 from German Collection of Microorganisms and Cell
111 Cultures, DSMZ) was cultured with thiosulfate in an anaerobic (pH 6.8) nutrient medium
112 specially designed for *T. denitrificans*, following Beller (2005). The medium consisted of a mixed
113 solution of $Na_2S_2O_3 \cdot 5H_2O$ (20 mM), NH_4Cl (18.7 mM), KNO_3 (20 mM), KH_2PO_4 (14.7 mM),
114 $NaHCO_3$ (30 mM), $MgSO_4 \cdot 7H_2O$ (3.25 mM), $FeSO_4 \cdot 7H_2O$ (0.08 mM), $CaCl_2 \cdot 2H_2O$ (0.05 mM)

and sterile vitamin, trace element and selenate-tungstate solutions. The cultures were maintained by 5-weekly sub-culturing, unshaken under anaerobic conditions at 30°C. 10 mL of growing culture were harvested by centrifugation at 3000 rpm for 15 min. The pellets were washed three times with sterile saline solution (Ringer 1/4 solution) and resuspended in 20 mL of the same solution immediately before the start of the experiments.

2.3. Experimental set-up

All experiments were performed in an anaerobic glove box with a nominal gas composition of 90% N_2 and 10% CO_2 at 28±2 °C. The oxygen partial pressure in the glove box was maintained between 0.1 and 0.3% O_2 and was continuously monitored by an oxygen partial pressure detector with an accuracy of ±0.1% O_2.

2.3.1. Batch experiments

Seven types of batch experiments were performed in sterilized 250 mL crystal Witeg bottles (Table 1). The sterilized control experiment (SC) was carried out adding sterilized core fragments and sterilized powdered pyrite to sterilized groundwater. The aim of this experiment was to evaluate potential pure chemical nitrate reduction. The natural control experiments (NC) consisted of core fragments and aquifer groundwater. In the unamended sterilized control experiments (USC), sterilized core fragments were added to sterilized groundwater. The objective of these experiments was to assess potential heterotrophic denitrification. The biostimulated experiments (B) were performed by amending with pyrite the core fragments and groundwater. The biostimulated and bioaugmented (BB) experiments were performed by inoculating with the *T. denitrificans* culture. The biostimulated and sterilized experiments (BS) were carried out with intact groundwater and sterilized core fragments amended with pyrite. The aim of these experiments was to assess relative contributions of solid-attached and free-living indigenous

bacteria to denitrification. Finally, the biostimulated, bioaugmented and sterilized experiments (BBS) consisted of sterilized core fragments and sterilized groundwater amended with pyrite and inoculated with the *T. denitrificans* culture. These experiments were performed to evaluate the denitrifying capacity of *T. denitrificans* in the absence of the indigenous bacterial community.

All experiments were run in duplicate with the exception of the sterilized control experiment. In the pyrite-amended experiments, pyrite was added in stoichiometric excess with respect to the initial nitrate concentration. Bottles were manually shaken once a day and aqueous samples (8 mL) were collected using sterile syringes at intervals of 1-4 weeks depending on denitrification dynamics. All experiments lasted 100 d.

Nitrate reduction rates were computed assuming zero-order kinetics and using linear regression to fit data of nitrate concentration vs. time. The same procedure was used to calculate sulfate production rates. Nitrate reduction and sulfate production rates were further normalized to the total mass of substrate (10 g).

2.3.2. Flow-through experiments

Two types of flow-through experiments were performed: ones using initial core fragments (8 g) and sterilized pyrite (2 g) to study the feasibility and long-term efficiency of the enhanced denitrification by pyrite addition; the second type, using the final solid material retrieved for the previous pyrite-amended batch experiments to evaluate the denitrifying long-term capacity of the bacterial consortium enriched therein.

The influent solution consisted of either groundwater from the aquifer or a sterilized modified medium solution with 2.5 mM NO_3^-. The modified medium was composed of 18.7 mM NH_4Cl, 14.7 mM KH_2PO_4, 30 mM $NaHCO_3$, 3.25 mM $MgCl_2 \cdot 6H_2O$, 0.05 mM $CaCl_2 \cdot 2H_2O$ and 2.5 mM KNO_3. This solution was sparged with N_2 for 15 min before sterilization.

The influent solutions were circulated through 50 mL polyethylene reactors by a peristaltic pump and the reactors were operated in an up-flow mode with a flow rate of 0.003-0.004 mL min^{-1}, which corresponds to a hydraulic retention time (HRT) of approximately 8-14 d. Experimental runs lasted 180 d, output solutions were collected once a week and chemical analyses were performed.

2.4. Chemical and isotopic analyses

Initial groundwater and aqueous samples collected during the experiments were analyzed to determine cation and anion concentrations, $\delta^{15}N$ and $\delta^{18}O$ of dissolved nitrate, alkalinity and pH. Sample aliquots were filtered through 0.22 μm syringe filters. For cation analyses, samples were acidified with 1% nitric acid and analyzed by inductively coupled plasma-atomic emission spectrometry (ICP-AES). The uncertainty in the measurement of Mg, Ca, Na, P, S, Fe and K was estimated to be around 5% based on replicate measurements, with detection limits of 2.06, 2.50, 4.35, 3.23, 3.12, 0.36 and 2.56 μM, respectively. Concentrations of nitrate, nitrite, chloride, and sulfate were determined by High Performance Liquid Chromatography (HPLC) using an IC-Pack Anion column and borate/gluconate eluent with 12% of HPLC grade acetonitrile. The error based on replicate measurements was 5% for nitrate, chloride and sulfate and 10% for nitrite. The sulfate concentrations measured by HPLC and those calculated from ICP sulfur elemental data were concordant within 5%, assuming that concentrations of non-sulfate sulfur species (sulfides and sulfites) were negligible. Samples for ammonium analysis were preserved acidified to pH<2 with H_2SO_4. Ammonium concentrations were measured using an Orion ammonium ion selective electrode with an analytical uncertainty of 10% and a detection limit of 0.01 mM. pH was measured with a calibrated Crison pH Meter at room temperature (22±2 °C). The pH error was

183 0.02 pH units. Alkalinity in unfiltered samples was measured by titration using an Aquamerck®
184 alkalinity test kit, with a detection limit of 0.1 meq L^{-1}.

185 Samples for N and O isotopes of nitrate were preserved with KOH (pH 11) and frozen prior
186 to analysis. The $\delta^{15}N$ and $\delta^{18}O$ of dissolved nitrate were obtained following the denitrifier method
187 (Casciotti et al., 2002; Sigman et al., 2001). Isotope compositions are reported on the usual δ-scale
188 in δ per mil relative to the international standards: V-SMOW (Vienna Standard Mean Oceanic
189 Water) for $\delta^{18}O$ and AIR (Atmospheric N_2) for $\delta^{15}N$. The isotope ratios were calculated using
190 international and internal laboratory standards. Precision (1σ) calculated from repeated analyses
191 of standards systematically interspersed in the analytical batches was 0.2 ‰ for $\delta^{15}N$ and 0.5 ‰
192 for $\delta^{18}O$ of nitrate. Each sample was analyzed in duplicate and the isotopic values are reported in
193 Table S1 (Supplementary data) as the average ± one standard deviation.

194 **2.5. Microbial community analysis**

195 **2.5.1. DNA extraction**

196 To extract total DNA from initial groundwater and from aqueous samples collected during
197 the experiments, biomass was concentrated by filtering through 0.22-μm cellulose acetate filters
198 (200 mL of groundwater or 50 mL of aqueous samples). Solid samples (0.25 g approximately)
199 were collected from the aquifer and at the end of the experiments for subsequent DNA extraction.
200 Total DNA was extracted in duplicate using a bead beating protocol by means of the commercial
201 PowerSoil™ DNA Isolation Kit (Mo-Bio). No further purification was required to prevent PCR
202 inhibition.

203 **2.5.2. PCR and Denaturing Gradient Gel Electrophoresis (DGGE)**

204 The V3-V5 variable regions of the *16S rRNA* gene were amplified using the primers 16F341-
205 GC and 16R907 (Yu and Morrison, 2004). Fragments of the *nosZ* gene were amplified using the

206 primers *NosZ*-F and *NosZ*1622R-GC (Kloos et al., 2001; Throbäck et al., 2004). All PCR reactions
207 were performed in a Mastercycler (Eppendorff). The PCR profile consisted in an initial
208 denaturation at 94°C for 5 min followed by 30 cycles of the following steps: a denaturation step at
209 94°C for 1 min, an annealing step at 55°C /53°C (*16S rRNA*/*nosZ*, respectively) for 1 min and an
210 elongation step at 72°C for 45 s. The last step involved an extension at 72°C for 10 min. Amplicons
211 were purified prior to the DGGE analysis using the DNA purification system Wizard® Plus SV
212 (Promega Corporation).

213 Approximately 800 ng of purified PCR products quantified using Nanodrop (ND-1000)
214 were loaded onto 8% (w/v) polyacrylamide gels (0.75 mm thick), with denaturing gradients
215 ranging from 30 to 70% (100% denaturant contains 7M urea and 40% (w/v) formamide). The
216 DGGE analyses were performed in a 1×TAE buffer solution (40 mM Tris, 20 mM sodium acetate,
217 1 mM EDTA, pH 7.4) using a DGGE-4001 System (CBS Scientific Company) at 100V and 60°C for
218 16 h. The DGGE gels were stained for 45 min in a 1×TAE buffer solution containing SybrGold
219 (Molecular Probes, Inc.) and then scanned under blue light by means of a Blue-converter plate
220 (UVP) and a UV Transilluminator (GeneFlash Synoptics Ltd). DGGE bands were processed using
221 the Gene Tools software v. 4.0 (SynGene Synoptics) and corrected manually.

222 Selected DGGE bands were removed with a sterile razor blade, resuspended in 50 μL
223 sterilized MilliQ water and stored at 4°C overnight. A 1:100 dilution of supernatant was used to
224 reamplify the *16S rRNA* DGGE bands with the primers 16F341-GC and 16R907 and PCR
225 conditions as described before. Finally, band amplicons were sequenced using the primer 16R907
226 without GC-clamp. Sequencing conditions consisted of an initial denaturation step at 96°C for 1
227 min, followed by 25 cycles of a denaturation step at 96°C for 10 s, an annealing step at 52.5°C for 5
228 s and an elongation step at 60°C for 4 min. The last step involved an extension at 72°C for 10 min.
229 Sequencing was performed using the ABI Prism Big Dye Terminator cycle-sequencing reaction

kit version 3.1 (Perkin-Elmer Applied Biosystems) and an ABI 3700 DNA sequencer (PE Applied Biosystems). Sequences were edited and assembled using version 7.0.9.0 of the BioEdit software (Hall, 1999) and were inspected for the presence of ambiguous base assignments. The sequences were then subjected to the Check Chimera program of the Ribosomal Database Project (Maidak et al., 2000) and aligned against GenBank database by using the alignment tool comparison software BLASTn and RDP search (Altschul et al., 1990; Maidak et al., 2000).

The *16S rRNA* gene nucleotide sequences determined in the present study were deposited into the GenBank database under accession numbers HM765437-HM765449.

2.5.3. Quantitative PCR assays

Two independent real-time qPCR reactions were performed for each gene (*16S rRNA* and *nosZ*), for each duplicate genomic DNA extraction. qPCR assays were run on a MX3000P Real Time PCR equipment (Stratagene) using a reaction volume of 25 µl by using SYBR® Green I qPCR Master Mix (Stratagene). Amplification of products was obtained by using the primers 519F/907R for the *16S rRNA* gene (Lane, 1991) and *nosZ*1F/*nosZ*1R for the *nosZ* gene (Kandeler et al., 2006). Thermal cycling conditions for the *nosZ*1 primers were as follows: an initial cycle at 95°C for 10 min followed by 40 cycles of 95°C for 30 s, 62°C for 1 min and 80°C for 15 s (fluorescence acquisition step). The thermocycling steps of the qPCR for *16S rRNA* amplification included an initial cycle at 95°C for 10 min and 40 cycles of 95°C for 30 s, 50°C for 30 s, 72°C for 45 s and 80°C for 15 s (fluorescence acquisition step). Product size and purity were confirmed by both melting-curve analysis (Mx3000P real-time PCR instrument software, version 4.0) and gel electrophoresis. Serial dilutions of total DNA extracts from sediment/water samples were quantified and compared to check for the potential presence of PCR inhibitors.

252 To perform calibration curves, standards were prepared with serial dilutions of a given
253 amount of environmental clone-plasmids containing PCR amplicons of the *16S rRNA* or the *nosZ*
254 gene. Standard curves obtained from both genes showed a linear range between 10^1 and 10^8 gene
255 copies reaction^{-1}, with slopes ranging from -3.3 to -3.5. The calculated PCR efficiencies for *16S*
256 *rRNA* and *nosZ* assays were 96 and 97%, respectively.

257 ## 3. RESULTS

258 ### 3.1. Batch experiments

259 Chemical and isotopic results of samples obtained from the batch experiments are detailed
260 in Table S1 (Supplementary data).

261 In the sterilized control experiment (SC), chemically-driven nitrate reduction did not occur
262 (Fig. 1A) and sulfate was released to solution (Fig. 1B). In the natural control and unamended
263 sterilized control experiments (NC and USC), no significant nitrate reduction occurred (Fig. 1A)
264 and no significant changes in alkalinity were observed. Between 0.1 and 0.2 mM sulfate was
265 produced in these unamended experiments (Table 2 and Fig. 1B), showing the dissolution of the
266 scarce pyrite present in the marl core fragments.

267 In the biostimulated experiments (B), initial nitrate concentration of 1.75 mM decreased to
268 less than 0.60 mM within 94 days (Fig. 1A). Ammonium concentration was below the detection
269 limit (0.01 mM). No transient nitrite accumulation occurred and sulfate was released to solution
270 (Fig. 1B). Total iron concentration was below the detection limit (0.36 μM). This suggests that
271 ferrous iron was also involved in nitrate reduction, being oxidized to ferric iron and precipitated
272 (solution pH ranged 6.8-7.2). The average nitrate reduction rate was 332±40 μmol NO_3^- kg^{-1} d^{-1}
273 (Table 2).

In the biostimulated and sterilized experiments (BS), both nitrate reduction and sulfate release occurred (Fig. 1A and 1B). The decrease in nitrate concentration and the release of sulfate were similar to those of the biostimulated experiments. The average nitrate reduction rate was also similar to that of the biostimulated experiments (361±11 μmol NO_3^- kg^{-1} d^{-1}, Table 2). In the biostimulated and bioaugmented experiments (BB), the variation of nitrate and sulfate concentrations was similar to that in the biostimulated experiments (Fig. 1A and 1B). Concentration of nitrite, ammonium and iron was below the detection limits, as in the biostimulated experiments. The average nitrate reduction rate was 383±47 μmol NO_3^- kg^{-1} d^{-1}, which is slightly higher than the rate obtained in the biostimulated experiments (Table 2).

In the experiments biostimulated, bioaugmented and sterilized (BBS), nitrate reduction and sulfate release also occurred (Fig. 1C and 1D). However, after 15 d in the BBS-1 experiment and after 29 d in the BBS-2 experiment, nitrate reduction ceased, with about 65% and 30% of the initial nitrate remaining in solution, respectively. The cessation of nitrate reduction was attributed to the decrease in pH to 6.2, which was low enough to affect activity of denitrifying bacteria (Torrentó et al., 2010). In the remaining experiments, pH was always higher than 6.5. In the BBS experiments, concentration of iron was also below the detection limit. Transient nitrite accumulation occurred during the first 45 d. Nevertheless, nitrite was completely removed after 70 d. The averaged nitrate reduction rate (1291±32 μmol NO_3^- kg^{-1} d^{-1}) was about a factor of 3 higher than those for the experiments with only indigenous bacteria (B and BS) and for the experiments with both indigenous and inoculated bacteria (BB).

Regardless of the behavior of nitrate, a significant amount of sulfate was produced during the first 4 d (between 1.6 and 4.6 mM, Table 2, Fig. 1B and 1D). Approximately 5 mM sulfate was also released in the sterilized control experiment during the first 4 d (Table 2 and Fig. 1B). This initial release of sulfate could be attributed to the pyrite's autoclaving process and/or the lysis of

298 the microbial population from the groundwater samples. Nevertheless, whatever led to this
299 initial jump in sulfate did not cause the release of sulfate after 4 d, since no sulfate was released in
300 the sterilized control experiment after 4 d (Table 2 and Fig. 1B). Therefore, the sulfate released
301 after 4 d can be clearly assigned to pyrite oxidation coupled to nitrate reduction. The sulfate
302 production rates were calculated using changes in the sulfate concentration measured after 4 d
303 (Table 2). In the case of the BBS-1 and BBS-2 experiments, the sulfate production rate was
304 calculated only from 4 d to 15 and 29 d, respectively, because nitrate reduction occurred only
305 during this period (Fig. 1C and 1D).

306 The ratio between the nitrate removal rate and the sulfate production rate (NO_3/SO_4) was
307 calculated for each pyrite-amended batch experiment (Table 2). Denitrification coupled to pyrite
308 oxidation is expressed as the following reaction, assuming a negligible accumulation of
309 intermediate N-gaseous products (e.g. NO and N_2O):

310 $$14NO_3^- + 5FeS_2 + 4H^+ \Rightarrow 7N_2 + 10SO_4^{2-} + 5Fe^{2+} + 2H_2O \quad (1)$$

311 If the Fe^{2+} produced is oxidized:

312 $$NO_3^- + 5Fe^{2+} + 6H^+ \Rightarrow \frac{1}{2}N_2 + 5Fe^{3+} + 3H_2O \quad (2)$$

313 an overall reaction is expressed as:

314 $$15NO_3^- + 5FeS_2 + 10H_2O \Rightarrow \frac{15}{2}N_2 + 5Fe(OH)_3 + 10SO_4^{2-} + 5H^+ \quad (3)$$

315 The measured NO_3/SO_4 ratio was compared with the stoichiometric molar ratio of the
316 overall reaction (eq. 3), which equals 1.5. In one experiment (B-2), the NO_3/SO_4 ratio was 1.2,
317 which is somewhat lower than the stoichiometric ratio. This was probably due to an excess of
318 sulfate (0.38 mM) that resulted from pyrite dissolution by traces of dissolved oxygen.
319 Nonetheless, in most of the experiments with indigenous bacteria (B, BS and BB), the NO_3/SO_4
320 ratios ranged between 1.5 and 2.0, suggesting that between 74 and 99% of nitrate reduction was

coupled to pyrite oxidation (Table 2). Furthermore, in the experiments with only inoculated bacteria (BBS), the ratio was 2.2 and 2.6, indicating that pyrite oxidation accounted for 59% and 70% of the nitrate reduction, respectively (Table 2). The residual fraction of nitrate reduced may be explained by heterotrophic denitrification.

3.2. Flow-through experiments

In all the flow-through experiments, complete nitrate removal was observed and pyrite dissolution was confirmed by sulfate release. The performance of one representative flow-through experiment as a function of time is illustrated in Fig. 2. In the experiments performed with initial core fragments complete nitrate removal was achieved after 14 d using groundwater as the influent and after 24 d using the sterilized 2.5 mM NO_3^- modified medium as the influent. In most of the flow-through experiments performed using the pyrite and aquifer material with attached biomass of autotrophically acclimated culture retrieved from previous batch experiments complete nitrate removal was achieved after 14 d. However, complete nitrate consumption was attained after 7 d in the experiments that were carried out using the material retrieved from the BB-1 and BB-2 batch experiments, respectively, which were initially inoculated with *T. denitrificans*.

The complete nitrate removal lasted for the 180-d test period and nitrite was only detected in the first samples where nitrate consumption was incomplete (Fig 2A). The output sulfate concentration was higher at the start of the experiments, subsequently decreasing until steady state was attained (Fig. 2B). This high concentration at the beginning of the experiments was probably due to the dissolution of an outer layer of the pyrite grains or to the dissolution of microparticles attached to pyrite surfaces (Lasaga, 1998). Iron concentrations were below the detection limit.

Considering the amounts of nitrate reduced and sulfate produced in the flow-through experiments, between 50 and 99% of the denitrification should be attributed to heterotrophic denitrifying bacteria in line with the stoichiometry of the overall pyrite-driven denitrification reaction (eq. 3).

3.3. Isotopic fractionation

During denitrification, as nitrate decreases, residual nitrate becomes enriched in the heavy isotopes ^{15}N and ^{18}O. The denitrification reaction describes a Rayleigh distillation process (eq. 4 and 5), where ε is the isotopic enrichment factor that depends on the aquifer materials and characteristics (Mariotti et al., 1981):

$$\delta^{15}N_{residual} = \delta^{15}N_{initial} + \varepsilon_N \ln f \quad (4)$$

$$\delta^{18}O_{residual} = \delta^{18}O_{initial} + \varepsilon_O \ln f \quad (5)$$

where f is the unreacted portion of nitrate (residual nitrate concentration divided by initial nitrate concentration), and $\delta_{residual}$ and $\delta_{initial}$ are the nitrogen or oxygen isotopic compositions (‰) of the residual and initial nitrate, respectively.

The N and O isotopic enrichment factors in two pyrite-amended batch experiments (biostimulated experiment B-2 and biostimulated and bioaugmented experiment BB-2) were calculated from the slope of the regression lines that fit the data of the natural logarithm of nitrate concentration vs. $\delta^{15}N$ or $\delta^{18}O_{NO3}$, respectively. The nitrogen isotopic enrichment factor (εN) was -27.6‰ and -25.0‰ for the B-2 and BB-2 experiments, respectively (Fig. 3A). The oxygen isotopic enrichment factor (εO) was -21.3‰ and -19.5‰, respectively (Fig. 3A) and the εN/εO ratios were 1.30 and 1.28, respectively (Fig. 3B).

The values of εN are within the range of denitrification enrichment factors attained from laboratory experiments with material from other aquifers (from -14.6‰ to -34.1‰; Grischek et al.,

1998; Sebilo et al., 2003; Tsushima et al., 2006; Table 3). To our knowledge, the O isotopic enrichment factors associated with denitrification and hence the εN/εO ratios have not been determined in the laboratory using aquifer sediments. The isotopic enrichment factors and the εN/εO ratios were therefore compared with those estimated for natural groundwater denitrification (see Table 3). In these *in situ* studies, the εN ranged from -57‰ (Singleton et al., 2007) to -4‰ (Fustec et al., 1991) and only three values of εO have been found: -8.0‰ (Böttcher et al., 1990), -9.8‰ (Fukada et al., 2003), and -18.3‰ (Mengis et al., 1999). The enrichment factors calculated in the present experiments are in general higher (in absolute value) than the ones reported in field studies, including the values estimated by Otero et al. (2009) for the Osona aquifer (Table 3). This difference is consistent with the commonly found discrepancy between enrichment factors for *in situ* studies and those for laboratory experiments. This divergence is attributed to the heterogeneity of aquifers, diversity of microbial communities, variations in temperature, variable presence of electron donors, and the occurrence in groundwater of other nitrate sinks (Mariotti et al., 1988).

The εN/εO ratios obtained in the present study are in agreement with reported ratios from *in situ* groundwater studies (Table 3) that range from 1.3 (Fukada et al., 2003) to 2.1 (Böttcher et al., 1990; Aravena and Robertson, 1998), and with those estimated by Otero et al. (2009) for the Osona aquifer (between 0.9 and 2.3, Table 3). Furthermore, the ratios are very close to the εN/εO ratio of 1.15 for pyrite-driven denitrification obtained in laboratory experiments with pure cultures of *T. denitrificans* (Torrentó et al., 2010).

3.4. PCR-DGGE analysis of the microbial community

The effects of the two bioremediation treatments on the aquifer bacterial community were analyzed by DGGE by using initial and final samples from the B-2 (biostimulated) and the BB-2 (biostimulated and bioaugmented) experiments.

Based on the visual comparison of the *16S rRNA*-based DGGE patterns before and after the experiments, both treatments produced changes in the composition of the dominant bacterial populations (Fig. 4). The DGGE banding pattern of original groundwater showed 5 faint bands (lane GW). Addition of pyrite or addition of pyrite and *T. denitrificans* resulted in the disappearance of these bands and in the appearance of novel predominant bands (lanes W-B and W-BB, respectively). A number of bands were common to the final aqueous samples of the two treatments (e.g. B10 and B25, B11 and B29, B13 and B30). However, other bands were unique to the biostimulated treatment (B14, B15 and B16) and to the biostimulated and bioaugmented experiment (B26-27 and B28). Selected bands were excised and sequenced and the taxonomic assignment of each excised band was performed (Table 4). The sequence analysis of the B10 and B25 bands indicated a 97% similarity with the *16S rRNA* gene of *Sediminibacterium sp.*, grouped with the *Bacteroidetes* phylum. The B11 and B29 bands were closely related to an unclassified *β-proteobacteria* of the *Methylophilaceae* family (96% similarity). The B30 band was related to an unclassified *γ-proteobacteria* closely related to the *Xanthomonadaceae* family (98% similarity).

The *16S rRNA*-based DGGE banding pattern of original aquifer sediment showed three intense bands, of which B7 band was the strongest (Fig. 4, lanes SED). The B20-B21 and B35-B36 bands from the solid sample retrieved at the end of the experiments (lanes S-B and S-BB) were in the same position as the B7 band. The *16S rRNA* gene from these bands (B7, B20 and B21) was identical to that of *Sphingomonas sp.*, within the *α-proteobacteria* class. At the end of the

experiments, most of the bands of the solid samples (lanes S-B and S-BB) were shared by the two treatments (e.g. B19 and B34, B20-21 and B35-36, B22 and B37, B23 and B38, B24 and B39). The B19 and B34 bands were in the same position as the B30 band from the final aqueous samples and were also identified as unclassified *γ-proteobacteria* closely related to the *Xanthomonadaceae* family. The *16S rRNA* sequence for the B39 band was consistent (99% similarity) with that found in an uncultured *Sideroxydans*, which belongs to the *β*-class of the *Proteobacteria*. The most important difference between the *16S rRNA*-based DGGE profiles of the two treatments was the appearance of the B40 band in the biostimulated and bioaugmented experiment (lanes S-BB). This band sequence was closely related to an uncultured *Methanogenium sp.* (99% similarity), grouped within the *Euryarchaeota* phylum.

Fig. S1 (Supplementary data) shows the *nosZ*-based DGGE profiles of the studied samples, which demonstrated that addition of pyrite also caused changes in the denitrifying community.

3.5. Quantification of *16S rRNA* and *nosZ* genes

qPCR assays were used to determine the copy number of *16S rRNA* and *nosZ* genes in the initial and final samples of the B-2 biostimulated experiment (Fig. 5). The addition of pyrite led to a significant increase in the number of *16S rRNA* gene copies in the solid samples, but not in the aqueous samples. Nevertheless, an increase in the number of *nosZ* copies was observed in both the sediment and the solution. The number of *nosZ* gene copies in the initial aquifer sediment was below the detection limit (approximately 10^3 *nosZ* copies g^{-1}). It should be noted that *16S rRNA* gene numbers from environmental samples cannot be converted to cell numbers as the exact number of copies of the *16S rRNA* gene in any given bacterial species varies, ranging from 1 to 13 (Fogel et al., 1999). In contrast to *16S rRNA*, only single copies per genome have been found for the denitrifying genes to date, except for the narG gene, which can be present in up to three

433 copies (Philippot, 2002). Therefore, the number of denitrifying organisms is expected to be close
434 to the gene copy number obtained by qPCR.

435 The ratio of the *nosZ* to *16S rRNA* genes was determined to evaluate the relative abundance
436 of denitrifiers compared to total bacteria. Such a calculation was possible for two reasons: a
437 similar amount of DNA was used (same DNA dilution without PCR inhibition for both genes)
438 and similar PCR efficiencies were obtained in the *16S rRNA* and *nosZ* assays. The percentage of
439 *nosZ* to *16S rRNA* genes in the initial groundwater sample was 1.3±0.5%, which is within the
440 range of those reported by Chon et al. (2011), Djigal et al. (2010), Henry et al. (2006) and Kandeler
441 et al. (2006) for environmental samples (0.1-4%). The relative abundance of the *nosZ* gene in
442 aqueous and solid samples increased from 1.34±0.46% before the experiment to 3.83±0.88% and
443 7.29±3.37%, respectively, after biostimulation.

444 **4. DISCUSSION**

445 **4.1. Enhancement of denitrification by pyrite addition and response of the microbial**
446 **community**

447 In the sterilized control, natural control and unamended sterilized control batch
448 experiments, insignificant nitrate reduction was observed, indicating a low background level of
449 electron donors needed for nitrate reduction in the aquifer material and the involvement of
450 bacteria in the denitrification processes. Nitrate reduction was enhanced in the experiments
451 amended with pyrite. This suggests that denitrifying bacteria capable of reducing nitrate using
452 pyrite as the electron donor were present in the aquifer material and that the addition of pyrite
453 was required to activate these autochthonous bacteria. The proportion of the *nosZ* gene
454 significantly increased after biostimulation in both aqueous and solid samples. It may be assumed

455 that the proportion of denitrifying bacteria increased, indicating that pyrite was used as the
456 electron donor in accordance with the nitrate consumption.

457 The DGGE fingerprint patterns showed that the composition of the bacterial community in
458 both the sediment and groundwater were highly affected by biostimulation. *γ-proteobacteria*
459 closely related to the *Xanthomonadaceae* family, *Sphingomonas* (*α-proteobacteria),* methylotrophic
460 bacteria (family *Methylophilaceae* of the *β-proteobacteria* class) and members of the *Bacteroidetes*
461 (family *Chitinophagaceae*) were probably responsible for denitrification in the present experiments.
462 In fact, in earlier studies, species belonging or closely related to these groups have been reported
463 as denitrifying bacteria (Cardenas et al., 2008; Finkmann et al., 2000; Ginige et al., 2004; Osaka et
464 al., 2006; Sahu et al., 2009; Sun et al., 2009). Members belonging to the *Sphingomonas*, *Bacteroidetes*
465 and *Methylophilaceae* could be affiliated with heterotrophic known denitrifying microorganisms.
466 *γ-proteobacteria* closely related to the *Xanthomonadaceae* family, detected both in water and
467 sediment, might be a good candidate for the pyrite-based denitrification. However, we do not
468 know whether it is the dominant autotrophic denitrifier capable of using pyrite as the electron
469 donor or other autotrophic denitrifying bacteria undetected by DGGE were present in the
470 community. This method is subject to shortcomings inherent to PCR-based techniques, such as
471 selectivity of DNA extraction or potential preferential amplification. Only bacterial populations
472 that make up 1% or more of the total community can be detected by DGGE (Muyzer et al., 1993;
473 Murray et al., 1996). Therefore, care should be taken with interpretation of DGGE results, as
474 major bands in the gels could not represent major populations in the environment (Muyzer and
475 Smalla, 1998).

476 Commonly, autotrophic denitrifiers are known as those bacteria able to couple the
477 oxidation of inorganic compounds, such as sulfide, iron, molecular hydrogen, uranium and other
478 metals, to the reduction of nitrate. It is noteworthy that the microbial diversity of autotrophic

denitrifiers in natural environments is not fully understood. In fact, several genes have been reported in the well known autotrophic denitrifier *Paracoccus denitrificans* that allows it to utilize both organic (methanol and methylamine) and inorganic substrates, being facultative heterotroph or autotroph (Winterstein and Ludwig, 1998).

Since organic carbon sources were not provided externally and no heterotrophic denitrification occurred in the natural control experiments, the dead and lysed cells of the autotrophic bacteria probably acted as the carbon source for the heterotrophic bacteria (Koenig et al., 2005; Torrentó et al., 2010). Therefore, the addition of pyrite to groundwater and sediment from the Osona aquifer stimulated both autotrophic and heterotrophic denitrifying bacteria. Accordingly, between 1 and 26% of the nitrate reduction must be attributed to heterotrophic bacteria so that the ratios between the nitrate removal rate and the sulfate production rate are consistent with the stoichiometry of the overall reaction (Table 2).

Surprisingly, although known denitrifying bacteria were detected among predominant *16S rRNA* gene-based DGGE bands, no *16S rRNA T. denitrificans* were detected in initial or final samples of the two treatments despite the fact that this bacterium is one of the most well known autotrophic denitrifier (Beller et al., 2006) and despite the fact that it has been shown to denitrify using pyrite as the electron donor (Torrentó et al., 2010). This would suggest that this bacterium was not the dominant denitrifier in the aquifer and that inoculated *T. denitrificans* was unable to compete with the indigenous bacteria for the electron acceptor and/or electron donor in the biostimulated and bioaugmented experiments, in agreement with the chemical results. Accordingly, in the *nosZ* DGGE profile (Fig. S1 in Supplementary data), although the bands were not successfully reamplified or sequenced, a very faint band (band 12, lanes W-BB) that was in the same position as the band for the *T. denitrificans* strain (band 16, lane TD) was detected in the final aqueous samples of the combined biostimulated and bioaugmented treatment but not in the

503 final samples of the biostimulated experiment (lanes W-B). Although inoculation with *T.*
504 *denitrificans* slightly accelerated nitrate reduction, bioaugmentation (at the inoculum density
505 tested in the present experiments) was thus not necessary to enhance denitrification. Even, the
506 *16S rRNA* DGGE profile of the biostimulated and bioaugmented experiment (Fig. 4, lanes S-BB)
507 showed the presence of methanogenic archaea (band B40), which were not clearly observed after
508 the biostimulation treatment. This would suggest that there was an excess of organic matter,
509 probably related to the biomass inoculated. Fermentation of such organic matter could take place,
510 generating hydrogen, which could be used by the methanogenic microbial populations as the
511 electron donor.

512 After biostimulation, the increase in the proportion of denitrifying bacteria was
513 significantly higher in the sediment-attached community than in the free-living community.
514 Nevertheless, in the biostimulated experiments that used sterilized core fragments (BS), the
515 nitrate reduction rate was similar to that obtained in the experiments that used non-sterilized core
516 fragments (B). Denitrifying bacteria existing in the aquifer groundwater were therefore able to
517 adapt to the new conditions and use pyrite as the electron donor even in the absence of viable
518 initial sediment-attached denitrifying bacteria. This assumption is concordant with the fact that
519 *Xanthomonadaceae*-like bacteria, which might probably be the dominant autotrophic denitrifiers in
520 the system, were detected in both solid and aqueous phases. The main phylogenetic difference
521 between the bacterial communities of aqueous and solid samples was the presence of
522 *Sphingomonas* in the solid samples, whereas the presence of *Bacteroidetes* and methylotrophic *β-*
523 *proteobacteria* was only detected in the aqueous samples.

524 The nitrate reduction rates obtained in the present batch experiments using the Osona
525 aquifer material biostimulated with pyrite (346±29 μmol NO_3^- kg^{-1} d^{-1}) were approximately 25
526 times higher than the rates obtained by Jorgensen et al. (2009) in pyrite-amended experiments

using sediments from the anoxic zone of a sandy aquifer (14±0.2 μmol NO_3^- kg^{-1} d^{-1}). After comparing experimental conditions in Jorgensen et al. (2009) with those in the present study, pyrite grain size, solid:liquid ratio and pH could account for this discrepancy in rates. Torrentó et al. (2010) demonstrated that the size of pyrite particles and pH significantly influenced nitrate removal rates and efficiency in pyrite-driven denitrification experiments with pure cultures of *T. denitrificans*. The discrepancies in nitrate reduction rates could be also due to differences in the capacity of the indigenous bacterial communities to respond to the addition of pyrite.

4.2. Long-term performance

In the flow-through experiments, nitrate reduction occurred concurrently with the release of sulfate. Complete nitrate removal commenced in the early stages of the experiments (less than 24 d) and lasted for the 180-d experimental period. This demonstrates the rapid response of the indigenous bacterial community to adapt to the new conditions and efficiently reduce nitrate. This result agrees with the high nitrate removal efficiency reported in Torrentó et al. (2010) for a long-term flow-through pyrite-amended experiment inoculated with *T. denitrificans*. In the present experiments, however, a shorter adaptation time was required for the bacteria to accomplish complete nitrate removal, thus providing evidence of the rapid adaptation of the native bacterial community to the addition of pyrite. The results demonstrated the long-term efficiency of enhanced denitrification by pyrite addition. This strategy could therefore be used in the field for the remediation of nitrate at the concentrations typically found in contaminated groundwater. As occurred in the batch experiments, pyrite addition probably stimulated both autotrophic and heterotrophic denitrifying bacteria. Given the lack of appropriate electron donors in the aquifer material, heterotrophic bacteria probably used dead and lysed cells of the

549 autotrophic bacteria as carbon source. In this case, most of the observed nitrate reduction must be
550 attributed to heterotrophic denitrification.

551 Therefore, results of both batch and flow-through experiments suggest that addition of
552 pyrite induced both autotrophic and heterotrophic denitrification. Autotrophic denitrification
553 dominated in the batch experiments, whereas heterotrophic denitrification was the dominant
554 process occurring in the flow-through experiments. In both types of experiments, pyrite addition
555 was necessary to activate indigenous heterotrophic and autotrophic denitrifying bacteria and
556 thus to enhance denitrification processes.

557 **4.3. Recalculation of the extent of natural attenuation in the Osona aquifer**

558 In most of the *in situ* groundwater studies, the N and/or O isotopic enrichment factors have
559 been calculated using chemical and isotopic compositions of groundwater sampled in multilevel
560 wells and/or in wells located along groundwater flux lines (Table 3). However, owing to the lack
561 of well casing and to the fact that sampling wells did not coincide with specific groundwater flow
562 directions, Otero et al. (2009) estimated εN and εO for the Osona aquifer using temporal
563 variations of nitrate concentration and $\delta^{15}N_{NO3}$ and $\delta^{18}O_{NO3}$ of a few wells in which denitrification
564 was prevalent during the period under study. The estimated enrichment factor for nitrogen
565 ranged between -4.4‰ and -15.5‰ with a median value of -7.0‰ and the εO ranged from -8.9‰
566 to -1.9‰ with a median value of -4.6‰.

567 Based on the *in situ* calculated εN and εO, Otero et al. (2009) roughly estimated the degree
568 of natural attenuation. The authors found a median percentage of denitrification of about 30%.
569 The isotopic enrichment factors derived from the present experiments using the Osona aquifer
570 material can be used to improve this estimation. The percentage of natural nitrate attenuation

was quantified in accordance with the following expression and using the εN and/or εO obtained in the experiments:

$$DEN(\%) = \left[1 - \frac{\left[NO_3^-\right]_{residual}}{\left[NO_3^-\right]_{initial}}\right] \times 100 = \left[1 - e^{\left(\frac{\delta_{(residual)} - \delta_{(initial)}}{\varepsilon}\right)}\right] \times 100 \quad (6)$$

The initial $\delta^{15}N_{NO3}$ and $\delta^{18}O_{NO3}$ values equal +15‰ and +5‰, respectively, which correspond to the isotopic composition of pig manure (Otero et al., 2009). Based on both the average εN= -26.3‰ and εO= -20.4‰, the degree of denitrification varied between 0 and 30%, except for sample MNL-019 that was higher than 50% (Fig. 6). The median percentage of denitrification was 10% (*n*=39) using εN= -26.3‰ and 7% (*n*=56) using εO= -20.4‰. It should be noted that since the isotopic enrichment factors used in the previous calculation were obtained from laboratory experiments, and since they are in general higher than those for *in situ* studies, a percentage of natural nitrate attenuation of at least about 10% is estimated for the Osona aquifer.

5. CONCLUSIONS

The present work evaluated the potential for removing nitrate from contaminated groundwater by stimulating the activity of denitrifying microorganisms by adding pyrite. The experiments demonstrated that (1) addition of pyrite (biostimulation) enhanced nitrate reduction, which reveals that pyrite addition was required to activate indigenous denitrifying microorganisms; (2) inoculation with *T. denitrificans* (bioaugmentation) was not necessary under the conditions of the present experiments.

Both autotrophic and heterotrophic denitrification was induced by pyrite addition. In those experiments amended with pyrite, the amount of sulfate produced accounted for more than 75% of the observed nitrate reduction. The addition of pyrite increased the proportion of denitrifying bacteria and led to a shift in the structure of the microbial community, stimulating not only

593 autotrophic but also heterotrophic denitrifying bacteria. Bacterial populations closely related to
594 *Xanthomonadaceae* might be a good candidate as the autotrophic denitrifier that used pyrite as the
595 electron donor. Nonetheless, direct evidence supporting this explanation should be confirmed by
596 further research. Heterotrophic denitrifying populations, such as members belonging to the
597 *Sphingomonas*, *Chitinophagaceae* and *Methylophilaceae*, were also stimulated through pyrite addition
598 and contributed to the overall denitrification.

599 The evolution of nitrate concentration and $\delta^{15}N$ and $\delta^{18}O$ of dissolved nitrate was consistent
600 with denitrification. The N and O isotopic enrichment factors were determined and used to
601 recalculate the extent of natural attenuation of nitrate in the Osona aquifer. The median
602 percentage of denitrification was around 10%, instead of the 30% that was previously
603 overestimated. This refinement could be useful in predicting the evolution of the nitrate
604 contamination in the aquifer and it should be taken into account for potential implementation of
605 induced remediation techniques.

606 Complete nitrate removal lasted for the 180-d test period in the flow-through experiments,
607 which demonstrated the durability of the effects of the bioremediation over time and the long-
608 term capacity of naturally occurring denitrifying bacteria to reduce nitrate.

609 Overall, these results suggest that controlled addition of pyrite to stimulate the activity of
610 indigenous denitrifying bacteria could be considered to remediate nitrate contamination in
611 groundwater in future water management strategies. However, a serious limitation of this
612 bioremediation strategy could be release of trace metals (e.g. As, Ni) and sulfate resulting from
613 the oxidation of pyrite (Torrentó et al., 2010). Further field-scale pilot plant studies are necessary
614 to test the practicability of this *in situ* bioremediation approach under natural conditions.

Acknowledgments. This work was funded by projects CICYT-CGL2008-06373-C03-01 and TRACE PET 2008-0034 of the Spanish Government and the project 2009 SGR 103 from the Catalan Government. We want to thank the Serveis Cientificotècnics of the Universitat de Barcelona, the GIRO Technological Centre and the Woods Hole Oceanographic Institution for their services. We wish to thank Vanessa Ouro, Josep Elvira, and Salvador Galí for analytical assistance and Albert Folch and Massimo Marchesi for their help during the sampling. We would like to thank Miriam Guivernau for analytical assistance in PCR-DGGE profiling and ribotype sequencing. We thank to George Von Knorring for improving the English style of this paper. We are grateful to Dr. Jeremy Fein and two anonymous reviewers for beneficial comments that increased the quality of the manuscript.

REFERENCES

Altschul, S.F., Gish, W., Miller, W., Myers, E.W., Lipman, D.J., 1990. Basic local alignment search tool. J. Mol. Biol. 215(3), 403-410.

Aravena, R., Robertson, W.D., 1998. Use of multiple isotope tracers to evaluate denitrification in ground water: Study of nitrate from a large-flux septic system plume. Ground Water 36(6), 975-981.

Beller, H.R., 2005. Anaerobic, nitrate-dependent oxidation of U(IV) oxide minerals by the chemolithoautotrophic bacterium *Thiobacillus denitrificans*. Appl. Environ. Microbiol. 71(4), 2170-2174.

Beller, H.R., Chain, P.S.G., Letain, T.E., Chakicherla, A., Larimer, F.W., Richardson, P.M., Coleman, M.A., Wood, A.P., Kelly, D.P., 2006. The genome sequence of the obligately chemolithoautotrophic, facultatively anaerobic bacterium *Thiobacillus denitrificans*. J. Bacteriol. 188(4), 1473-1488.

Böttcher, J., Strebel, O., Voerkelius, S., Schmidt, H.L., 1990. Using isotope fractionation of nitrate nitrogen and nitrate oxygen for evaluation of microbial denitrification in a sandy aquifer. J. Hydrol. 114(3-4), 413-424.

Cardenas, E., Wu, W.M., Leigh, M.B., Carley, J., Carroll, S., Gentry, T., Luo, J., Watson, D., Gu, B., Ginder-Vogel, M., et al., 2008. Microbial communities in contaminated sediments, associated with bioremediation of uranium to submicromolar levels. Appl. Environ. Microbiol. 74(12), 3718-3729.

Casciotti, K.L., Sigman, D.M., Hastings, M.G., Bohlke, J.K., Hilkert, A., 2002. Measurement of the oxygen isotopic composition of nitrate in seawater and freshwater using the denitrifier method. Anal. Chem. 74(19), 4905-4912.

Cey, E.E., Rudolph, D.L., Aravena, R., Parkin, G., 1999. Role of the riparian zone in controlling the distribution and fate of agricultural nitrogen near a small stream in southern Ontario. J. Contam. Hydrol. 37(1-2), 45-67.

Clément, J.C., Holmes, R.M., Peterson, B.J., Pinay, G., 2003. Isotopic investigation of denitrification in a riparian ecosystem in western France. J. Appl. Ecol. 40(6), 1035-1048.

Chon, K., Chang, J.S., Lee, E., Lee, J., Ryu, J., Cho, J., 2011. Abundance of denitrifying genes coding for nitrate (narG), nitrite (nirS), and nitrous oxide (nosZ) reductases in estuarine versus wastewater effluent-fed constructed wetlands. Ecol. Eng. 37(1), 64-69.

Della Rocca, C., Belgiorno, V., Meriç, S., 2007. Overview of in-situ applicable nitrate removal processes. Desalination 204(1-3), 46-62.

Devito, K.J., Fitzgerald, D., Hill, A.R., Aravena, R., 2000. Nitrate dynamics in relation to lithology and hydrologic flow path in a river riparian zone. J. Environ. Qual. 29(4), 1075-1084.

Djigal, D., Baudoin, E., Philippot, L., Brauman, A., Villenave, C., 2010. Shifts in size, genetic structure and activity of the soil denitrifier community by nematode grazing. Eur. J. Soil. Biol. 46(2), 112-118.

Finkmann, W., Altendorf, K., Stackebrandt, E., Lipski, A., 2000. Characterization of N_2O-producing *Xanthomonas*-like isolates from biofilters as *Stenotrophomonas nitritireducens* sp. nov., *Luteimonas mephitis* gen. nov., sp. nov. and *Pseudoxanthomonas broegbernensis* gen. nov., sp. nov. Int. J. Syst. Evol. Microbiol. 50(1), 273-282.

Fogel, G.B., Collins, C.R., Li, J., Brunk, C.F., 1999. Prokaryotic genome size and SSU rDNA copy number: Estimation of microbial relative abundance from a mixed population. Microb. Ecol. 38(2), 93-113.

Fukada, T., Hiscock, K.M., Dennis, P.F., Grischek, T., 2003. A dual isotope approach to identify denitrification in groundwater at a river-bank infiltration site. Water Res. 37(13), 3070-3078.

Fustec, E., Mariotti, A., Grillo, X., Sajus, J., 1991. Nitrate removal by denitrification in alluvial ground water: Role of a former channel. J. Hydrol. 123(3-4), 337-354.

Ginige, M.P., Hugenholtz, P., Daims, H., Wagner, M., Keller, J., Blackall, L.L., 2004. Use of Stable-Isotope Probing, full-cycle rRNA analysis, and Fluorescence In Situ Hybridization-Microautoradiography to study a methanol-fed denitrifying microbial community. Appl. Environ. Microbiol. 70(1), 588-596.

Grischek, T., Hiscock, K.M., Metschies, T., Dennis, P.F., 1998. Factors affecting denitrification during infiltration of river water into a sand and gravel aquifer in Saxony, Germany. Water Res. 32(2), 450-460.

Hall, T.A., 1999. BioEdit: A user-friendly biological sequence alignment editor and analysis program for Windows 95/98/NT. Nucleic Acids Symp. Ser. 41, 95-98.

Henry, S., Bru, D., Stres, B., Hallet, S., Philippot, L., 2006. Quantitative detection of the nosZ gene, encoding nitrous oxide reductase, and comparison of the abundances of 16S rRNA, narG, nirK, and nosZ genes in soils. Appl. Environ. Microbiol. 72(8), 5181-5189.

687 Jorgensen, C.J., Jacobsen, O.S., Elberling, B., Aamand, J., 2009. Microbial oxidation of pyrite
688 coupled to nitrate reduction in anoxic groundwater sediment. Environ. Sci. Technol. 43(13),
689 4851-4857.

690 Kandeler, E., Deiglmayr, K., Tscherko, D., Bru, D., Philippot, L., 2006. Abundance of narG, nirS,
691 nirK, and nosZ genes of denitrifying bacteria during primary successions of a glacier
692 foreland. Appl. Environ. Microbiol. 72(9), 5957-5962.

693 Kloos, K., Mergel, A., Rösch, C., Bothe, H., 2001. Denitrification within the genus *Azospirillum* and
694 other associative bacteria. Funct. Plant Biol. 28(9), 991-998.

695 Koenig, A., Zhang, T., Liu, L., Fang, H., 2005. Microbial community and biochemistry process in
696 autosulfurotrophic denitrifying biofilm. Chemosphere 58(8), 1041-1047.

697 Lane, D.J., 1991. 16S/23S rRNA sequencing, in: Stackebrandt, E., Goodfellow, M. (Eds.), Nucleic
698 Acid Techniques in Bacterial Systematics. Modern Microbiological Methods Series. Wiley,
699 New York, pp. 115-175.

700 Larsen, F., Postma, D., 1997. Nickel mobilization in a groundwater well field: Release by pyrite
701 oxidation and desorption from manganese oxides. Environ. Sci. Technol. 31(9), 2589-2595.

702 Lasaga, A.C., 1998. Kinetic Theory in the Earth Sciences. Princeton University Press, Princeton,
703 New Jersey, 728 pp.

704 Maidak, B.L., Cole, J.R., Lilburn, T.G., Parker, C.T., Saxman, P.R., Stredwick, J.M., Garrity, G.M.,
705 Li, B., Olsen, G.J., Pramanik, S., et al., 2000. The RDP (Ribosomal Database Project)
706 continues. Nucleic Acids Res. 28(1), 173-174.

707 Mariotti, A., Germon, J.C., Hubert, P., Kaiser, P., Létolle, R., Tardieux, A., Tardieux, P., 1981.
708 Experimental determination of nitrogen kinetic isotope fractionation - Some principles -
709 Illustration for the denitrification and nitrification processes. Plant Soil 62(3), 413-430.

710 Mariotti, A., Landreau, A., Simon, B., 1988. ^{15}N isotope biogeochemistry and natural
711 denitrification process in groundwater: application to the chalk aquifer of northern France.
712 Geochim. Cosmochim. Acta 52(7), 1869-1878.

713 Menció, A., Mas-Pla, J., Otero, N., Soler, A., 2010. Nitrate as a tracer of groundwater flow in a
714 fractured multilayered aquifer. Hydrolog. Sci. J., submitted.

715 Mengis, M., Schif, S.L., Harris, M., English, M.C., Aravena, R., Elgood, R.J., MacLean, A., 1999.
716 Multiple geochemical and isotopic approaches for assessing ground water NO_3 elimination
717 in a riparian zone. Ground Water 37(3), 448-457.

718 Murray, A.E., Hollibaugh, J.T., Orrego, C., 1996. Phylogenetic compositions of bacterioplankton
719 from two California estuaries compared by denaturing gradient gel electrophoresis of 16S
720 rDNA fragments. Appl. Environ. Microbiol. 62(7), 2676-2680.

721 Muyzer, G., De Waal, E.C., Uitterlinden, A.G., 1993. Profiling of complex microbial populations
722 by denaturing gradient gel electrophoresis analysis of polymerase chain reaction-amplified
723 genes coding for 16S rRNA. Appl. Environ. Microbiol. 59(3), 695-700.

724 Muyzer, G., Smalla, K., 1998. Application of denaturing gradient gel electrophoresis (DGGE) and
725 temperature gradient gel electrophoresis (TGGE) in microbial ecology. Anton. Leeuw. Int. J.
726 G. 73(1), 127-141.

727 Osaka, T., Yoshie, S., Tsuneda, S., Hirata, A., Iwami, N., Inamori, Y., 2006. Identification of
728 acetate- or methanol-assimilating bacteria under nitrate-reducing conditions by stable-
729 isotope probing. Microb. Ecol. 52(2), 253-266.

730 Otero, N., Torrentó, C., Soler, A., Menció, A., Mas-Pla, J., 2009. Monitoring groundwater nitrate
731 attenuation in a regional system coupling hydrogeology with multi-isotopic methods: The
732 case of Plana de Vic (Osona, Spain). Agr. Ecosyst. Environ. 133(1-2), 103-113.

733 Pauwels, H., Foucher, J.C., Kloppmann, W., 2000. Denitrification and mixing in a schist aquifer:
734 influence on water chemistry and isotopes. Chem. Geol. 168(3-4), 307-324.

735 Philippot, L., 2002. Denitrifying genes in bacterial and Archaeal genomes. Biochim. Biophys. Acta
736 Gene Struct. Expression 1577(3), 355-376.

737 Postma, D., Boesen, C., Kristiansen, H., Larsen, F., 1991. Nitrate reduction in an unconfined sandy
738 aquifer - Water chemistry, reduction processes and geochemical modeling. Water Resour.
739 Res. 27(8), 2027-2045.

740 Sahu, A.K., Conneely, T., Nüsslein, K., Ergas, S.J., 2009. Hydrogenotrophic denitrification and
741 perchlorate reduction in ion exchange brines using membrane biofilm reactors. Biotechnol.
742 Bioeng. 104(3), 483-491.

743 Sebilo, M., Billen, G., Grably, M., Mariotti, A., 2003. Isotopic composition of nitrate-nitrogen as a
744 marker of riparian and benthic denitrification at the scale of the whole Seine River system.
745 Biogeochemistry 63(1), 35-51.

746 Sigman, D.M., Casciotti, K.L., Andreani, M., Barford, C., Galanter, M., Bohlke, J.K., 2001. A
747 bacterial method for the nitrogen isotopic analysis of nitrate in seawater and freshwater.
748 Anal. Chem. 73(17), 4145-4153.

749 Singleton, M.J., Esser, B.K., Moran, J.E., Hudson, G.B., McNab, W.W., Harter, T., 2007. Saturated
750 zone denitrification: Potential for natural attenuation of nitrate contamination in shallow
751 groundwater under dairy operations. Environ. Sci. Technol. 41(3), 759-765.

752 Smith, R.L., Howes, B.L., Duff, J.H., 1991. Denitrification in nitrate-contaminated groundwater -
753 Occurrence in steep vertical geochemical gradients. Geochim. Cosmochim. Acta 55(7), 1815-
754 1825.

755 Smolders, A.J.P., Lamers, L.P.M., Lucassen, E.C.H.E.T., Van Der Velde, G., Roelofs, J.G.M., 2006.
756 Internal eutrophication: How it works and what to do about it - A review. Chem. Ecol.
757 22(2), 93-111.

758 Smolders, A.J.P., Lucassen, E.C.H.E.T., Bobbink, R., Roelofs, J.G.M., Lamers, L.P.M., 2010. How
759 nitrate leaching from agricultural lands provokes phosphate eutrophication in groundwater
760 fed wetlands: The sulphur bridge. Biogeochemistry 98(1-3), 1-7.

761 Soares, M.I.M., 2000. Biological denitrification of groundwater. Water Air Soil Pollut. 123(1-4),
762 183-193.

763 Spalding, R.F., Parrott, J.D., 1994. Shallow groundwater denitrification. Sci. Total Environ. 141(1-
764 3), 17-25.

765 Sun, W., Sierra-Alvarez, R., Milner, L., Oremland, R., Field, J.A., 2009. Arsenite and ferrous iron
766 oxidation linked to chemolithotrophic denitrification for the immobilization of arsenic in
767 anoxic environments. Environ. Sci. Technol. 43(17), 6585-6591.

768 Throbäck, I.N., Enwall, K., Jarvis, A., Hallin, S., 2004. Reassessing PCR primers targeting nirS,
769 nirK and nosZ genes for community surveys of denitrifying bacteria with DGGE. FEMS
770 Microbiol. Ecol. 49(3), 401-417.

771 Torrentó, C., Cama, J., Urmeneta, J., Otero, N., Soler, A., 2010. Denitrification of groundwater
772 with pyrite and *Thiobacillus denitrificans*. Chem. Geol., 278(1-2): 80-91.

773 Tsushima, K., Ueda, S., Ogura, N., 2002. Nitrate loss for denitrification during high frequency
774 research in floodplain groundwater of the Tama River. Water Air Soil Pollut. 137(1-4), 167-
775 178.

776 Tsushima, K., Ueda, S., Ohno, H., Ogura, N., Katase, T., Watanabe, K., 2006. Nitrate decrease with
777 isotopic fractionation in riverside sediment column during infiltration experiment. Water
778 Air Soil Pollut. 174(1-4), 47-61.

779 Vitòria, L., Soler, A., Canals, A., Otero, N., 2008. Environmental isotopes (N, S, C, O, D) to
780 determine natural attenuation processes in nitrate contaminated waters: Example of Osona
781 (NE Spain). Appl. Geochem. 23(12), 3597-3611.

782 Vogel, T.M., 1996. Bioaugmentation as a soil bioremediation approach. Curr. Opin. Biotechnol.
783 7(3), 311-316.

784 Wang, Q., Garrity, G.M., Tiedje, J.M., Cole, J.R., 2007. Naïve Bayesian classifier for rapid
785 assignment of rRNA sequences into the new bacterial taxonomy. Appl. Environ. Microbiol.
786 73(16), 5261-5267.

787 Ward, M.H., deKok, T.M., Levallois, P., Brender, J., Gulis, G., Nolan, B.T., VanDerslice, J., 2005.
788 Workgroup report: Drinking-water nitrate and health-recent findings and research needs.
789 Environ. Health Perspect. 113(11), 1607-1614.

790 Winterstein, C., Ludwig, B., 1998. Genes coding for respiratory complexes map on all three
791 chromosomes of the *Paracoccus denitrificans* genome. Arch. Microbiol. 169(4), 275-281.

792 Yu, Z., Morrison, M., 2004. Comparisons of different hypervariable regions of rrs genes for use in
793 fingerprinting of microbial communities by PCR-denaturing gradient gel electrophoresis.
794 Appl. Environ. Microbiol. 70(8), 4800-4806.

795 Zumft, W.G., 1997. Cell biology and molecular basis of denitrification. Microbiol. Mol. Biol. Rev.
796 61(4), 533-616.

Figure captions

Figure 1. Variation of nitrate and sulfate concentration over time in batch experiments. (A) Nitrate and (B) sulfate concentration vs. time in the sterilized control (SC), the natural control (NC), the unamended sterilized control (USC), the biostimulated (B), the biostimulated and sterilized (BS) and the biostimulated and bioaugmented (BB) experiments; Variation of (C) nitrate concentration and (D) sulfate concentration over time in the biostimulated, bioaugmented and sterilized experiments (BBS). Lines represent the fit of measured nitrate and sulfate concentration vs. time used to compute zero-order nitrate reduction and sulfate production rates, respectively (see Table 2).

Figure 2. Variation of (A) nitrate and nitrite concentrations and (B) sulfate concentration over time in one representative flow-through experiment. The inset in Fig. 2B shows in more detail how sulfate concentration decreases over time until steady state close to the detection limit is attained. The sulfate detection limit (3.12 μM) is indicated by the dotted line.

Figure 3. (A) $\delta^{15}N_{NO3}$ and $\delta^{18}O_{NO3}$ vs. ln $[NO_3^-]$ of the B-2 (biostimulated) and BB-2 (biostimulated and bioaugmented) pyrite-amended batch experiments. Values of εN and εO were obtained from the slope of the regression lines. (B) $\delta^{18}O_{NO3}$ vs. $\delta^{15}N_{NO3}$ of the same B-2 and BB-2 experiments.

Figure 4. DGGE profiles of PCR-amplified *16S rRNA* genes (V3-V5 hypervariable region) from the studied samples. TD: *T. denitrificans* strain; GW: original aquifer groundwater; SED: original aquifer sediment; W-B: aqueous sample at the end of the B-2 biostimulated experiment; S-B: solid sample at the end of the B-2 biostimulated experiment; W-BB: aqueous sample at the end of the BB-2 biostimulated and bioaugmented experiment; S-BB: solid sample at the end of the

819 BB-2 biostimulated/bioaugmented experiment. The DGGE analyses were reproducible since no
820 variations were observed between the patterns obtained from duplicate DNA extractions.

821 **Figure 5**. *16S rRNA* and *nosZ* genes copy numbers in aqueous samples (gene copies mL^{-1}) or
822 in sediment (gene copies g^{-1}). Abbreviations are the same as in Fig. 4. Error bars indicate standard
823 deviations of qPCR of the two replicate DNA extractions.

824 **Figure 6**. $\delta^{15}N$ vs. $\delta^{18}O_{NO3}$ of the Osona groundwater used to estimate the percentage of
825 natural denitrification, quantified in terms of the isotope enrichment factors obtained in the
826 present experiments (median values are used: εN= -26.3‰ and εO= -20.4‰). The ranges of
827 denitrification percentages calculated using these εN and εO values are shown.

Figure 1

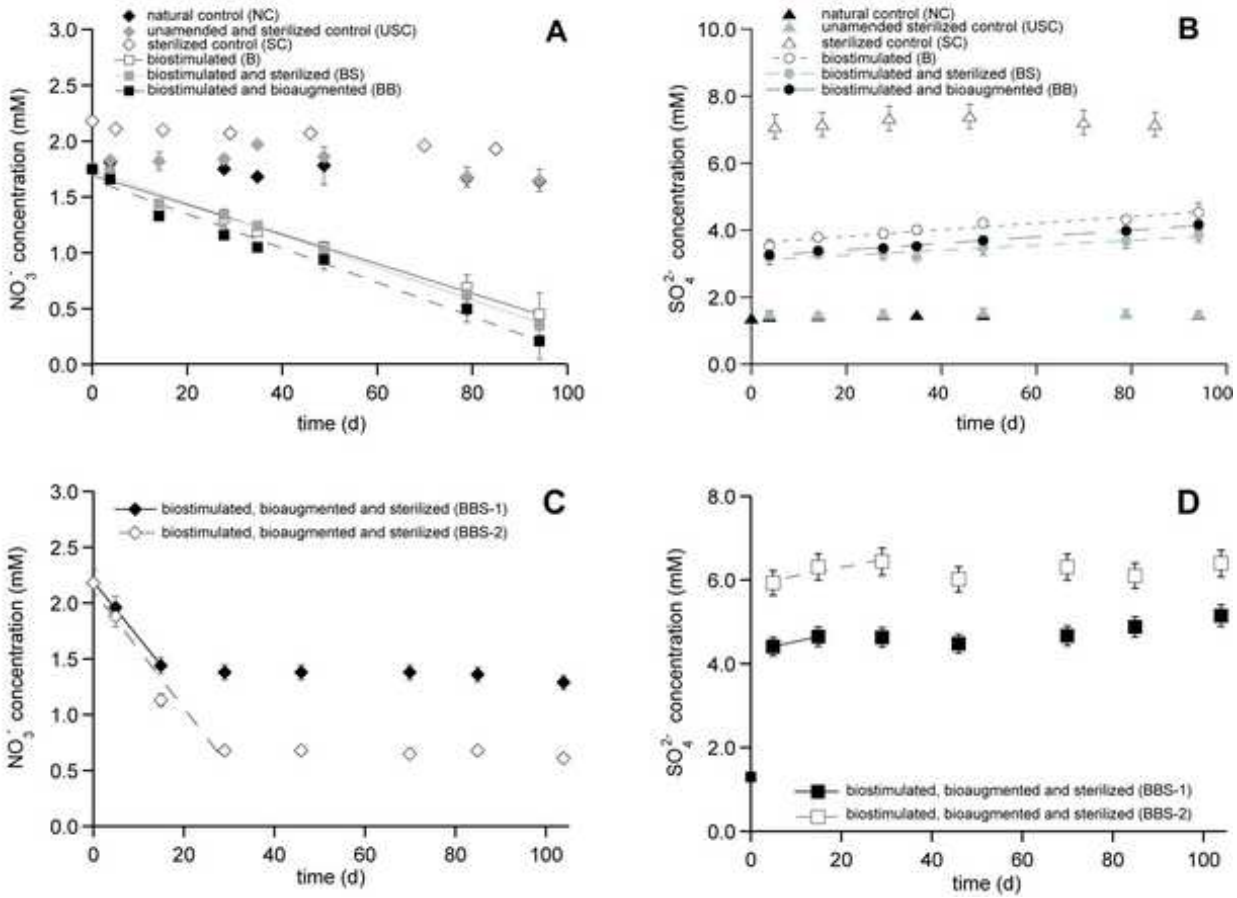
A
natural control (NC)
unamended and sterilized control (USC)
sterilized control (SC)
biostimulated (B)
biostimulated and sterilized (BS)
biostimulated and bioaugmented (BB)
NO_3^- concentration (mM)
time (d)
B
natural control (NC)
unamended sterilized control (USC)
sterilized control (SC)
biostimulated (B)
biostimulated and sterilized (BS)
biostimulated and bioaugmented (BB)
SO_4^{2-} concentration (mM)
time (d)
C
biostimulated, bioaugmented and sterilized (BBS-1)
biostimulated, bioaugmented and sterilized (BBS-2)
NO_3^- concentration (mM)
time (d)
D
biostimulated, bioaugmented and sterilized (BBS-1)
biostimulated, bioaugmented and sterilized (BBS-2)
SO_4^{2-} concentration (mM)
time (d)

Figure 2

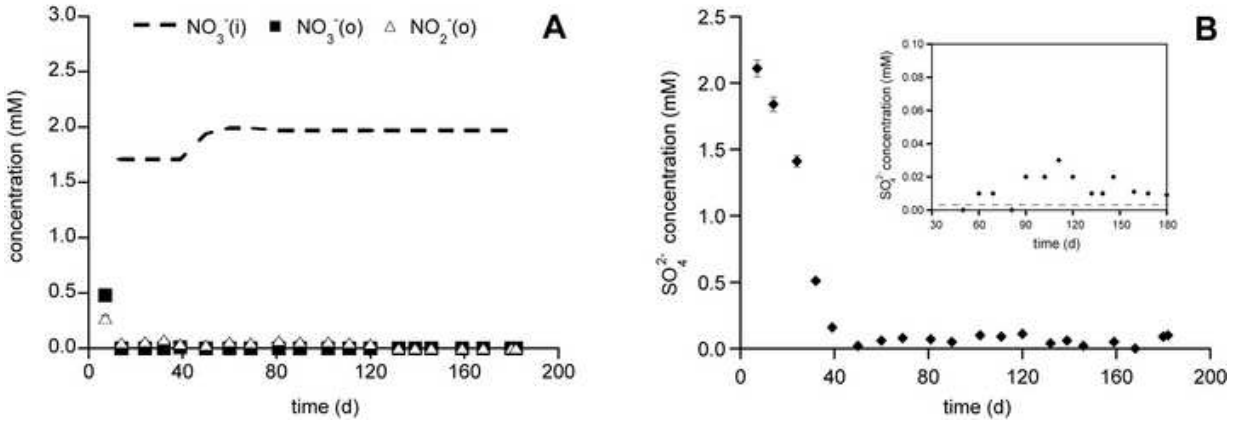
A
NO_3^-(i)
NO_3^-(o)
NO_2^-(o)
concentration (mM)
time (d)
B
SO_4^{2-} concentration (mM)
SO_4^{2-} concentration (mM)
time (d)
time (d)

Figure 3

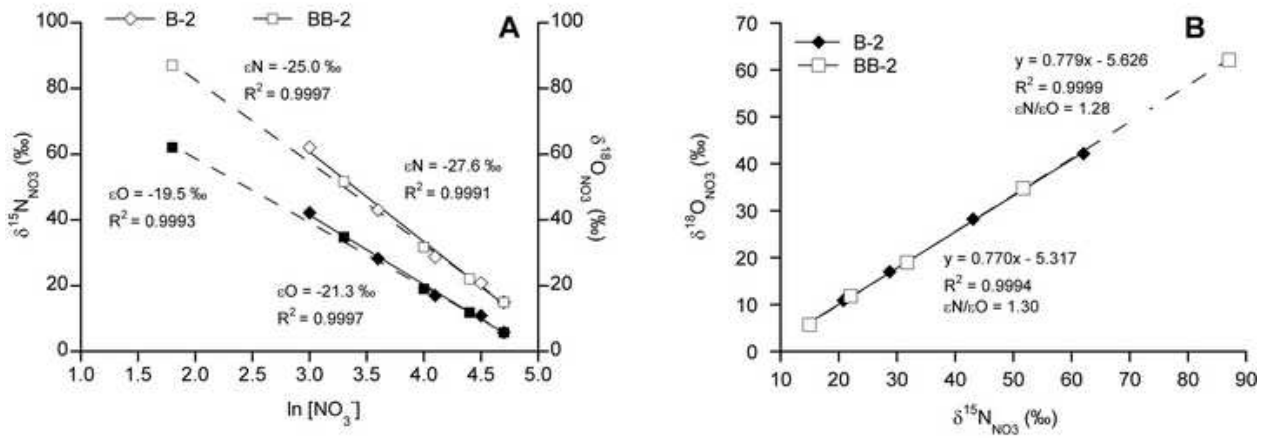
A
B-2
BB-2
εN = -25.0 ‰
R² = 0.9997
εN = -27.6 ‰
R² = 0.9991
εO = -19.5 ‰
R² = 0.9993
εO = -21.3 ‰
R² = 0.9997
δ15NNO3 (‰)
δ18ONO3 (‰)
ln [NO3-]
B
B-2
BB-2
y = 0.779x - 5.626
R² = 0.9999
εN/εO = 1.28
y = 0.770x - 5.317
R² = 0.9994
εN/εO = 1.30
δ18ONO3 (‰)
δ15NNO3 (‰)

Figure 4

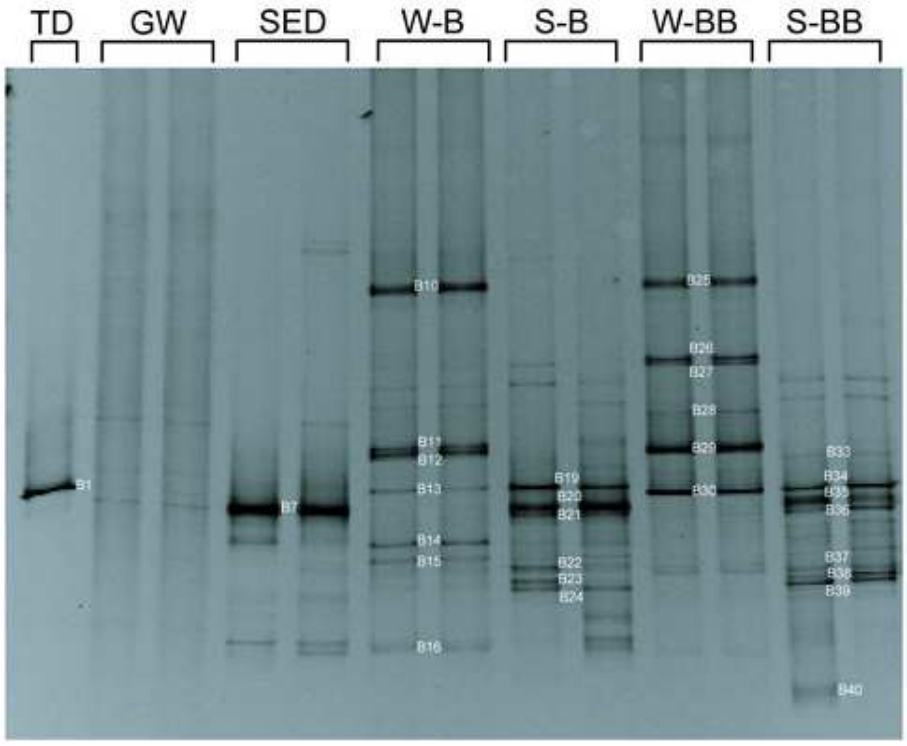
TD
GW
SED
W-B
S-B
W-BB
S-BB
B1
B7
B10
B11
B12
B13
B14
B15
B16
B19
B20
B21
B22
B23
B24
B25
B26
B27
B28
B29
B30
B33
B34
B35
B36
B37
B38
B39
B40

Figure 5

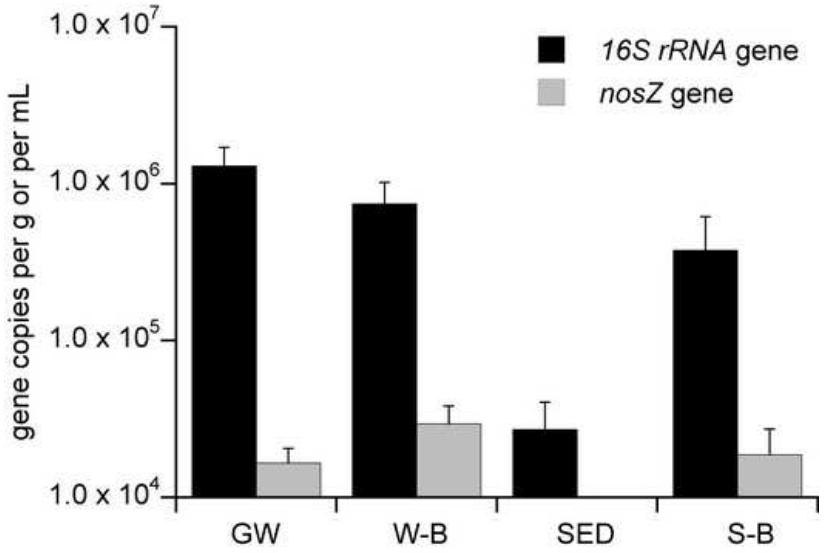
1.0 x 10^7
1.0 x 10^6
1.0 x 10^5
1.0 x 10^4
gene copies per g or per mL
16S rRNA gene
nosZ gene
GW
W-B
SED
S-B

Figure 6

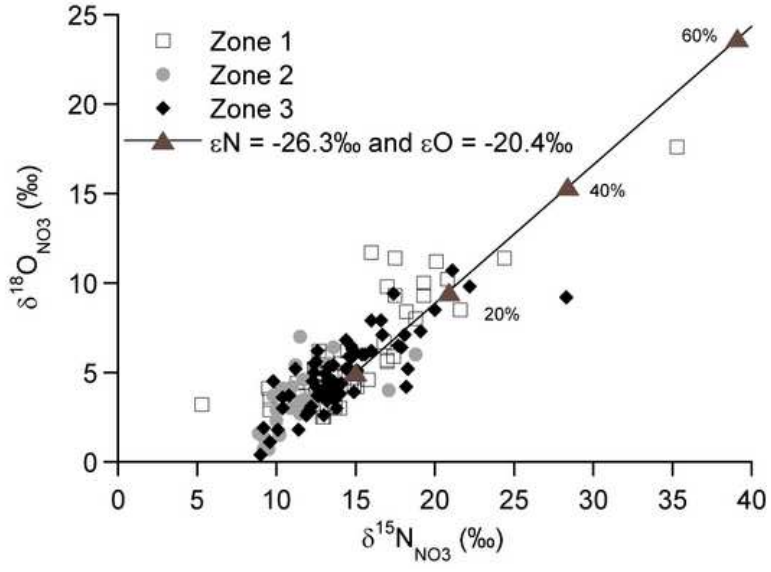
Zone 1
Zone 2
Zone 3
εN = -26.3‰ and εO = -20.4‰
60%
40%
20%
δ18ONO3 (‰)
δ15NNO3 (‰)
0
5
10
15
20
25
30
35
40

Table 1. Experimental conditions of the batch experiments

Code	Experiments	Contents of the incubation
SC	sterilized control	8 g sterilized core fragments, 250 mL sterilized groundwater, 2 g sterilized pyrite
NC	natural control	10 g core fragments, 250 mL groundwater
USC	unamended sterilized control	10 g sterilized core fragments, 250 mL sterilized groundwater
B	biostimulated	8 g core fragments, 250 mL groundwater, 2 g sterilized pyrite
BS	biostimulated and sterilized	8 g sterilized core fragments, 250 mL groundwater, 2 g sterilized pyrite
BB	biostimulated and bioaugmented	8 g core fragments, 250 mL groundwater, 2 g sterilized pyrite, 8 mL *T. denitrificans* culture (6.6×10^{7} cells mL^{-1})
BBS	biostimulated, bioaugmented and sterilized	8 g sterilized core fragments, 250 mL sterilized groundwater, 2 g sterilized pyrite, 8 mL *T. denitrificans* culture (1.2×10^{8} cells mL^{-1})

Table 2. Nitrate reduction and sulfate production in the batch experiments

Experiment	*T. den.* inoculum	Nitrate reduction rate [a]		Nitrate reduced	Sulfate produced (0-4 d)	Sulfate produced (4 d-end)	Sulfate production rate [b]		NO_3 reduction rate / SO_4 production rate	% of nitrate reduction related to pyrite oxidation [c]
	Cells mL^{-1}	µmol NO_3^- kg^{-1} d^{-1}	R^2	mM	mM	mM	µmol SO_4^{2-} kg^{-1} d^{-1}	R^2		
Sterilized control										
SC	-	-	-	-	5.06	-	-	-	-	-
Natural control										
NC-1	-	-	-	-	0.04	-	-	-	-	-
NC-2	-	-	-	-	0.06	-	-	-	-	-
Unamended sterilized control										
USC-11	-	-	-	-	0.04	-	-	-	-	-
USC-12	-	-	-	-	0.20	-	-	-	-	-
Biostimulated										
B-1	-	303	0.970	1.17	2.31	0.63	180	0.944	1.7	89
B-2	-	360	0.989	1.43	2.02	1.34	311	0.914	1.2	130
mean±SD		332±40		1.30±0.19	2.17±0.20	0.98±0.50	246±93		1.4±0.4	109±29
Biostimulated and sterilized										
BS-1	-	353	0.993	1.37	1.66	0.70	174	0.947	2.0	74
BS-2	-	368	0.992	1.42	1.95	0.69	189	0.992	1.9	77
mean±SD		361±11		1.39±0.04	1.80±0.20	0.69±0.01	182±10		2.0±0.1	76±2
Biostimulated and bioaugmented										
BB-1	6.6×10^7	350	0.971	1.43	1.88	0.81	216	0.992	1.6	93
BB-2	6.6×10^7	416	0.987	1.65	1.91	0.97	273	0.989	1.5	99
mean±SD		383±47		1.54±0.16	1.90±0.02	0.89±0.12	245±40		1.6±0.1	96±4
Biostimulated, bioaugmented and sterilized										
BBS-1	1.2×10^8	1268	0.998	0.75	3.04	0.24	590	-	2.1	70
BBS-2	1.2×10^8	1314	0.960	1.50	4.56	0.51	514	0.868	2.6	59
mean±SD		1291±32		1.12±0.53	3.80±1.07	0.37±0.20	552±54		2.4±0.3	64±8

[a] In the BBS-1 and BBS-2 experiments, nitrate reduction rates were calculated during the first 15 and 29 d, respectively. Afterwards, nitrate reduction ceased (see text)

[b] Sulfate production rate was calculated from 4 d to the end of the experiments, except for the BBS-1 and BBS-2 experiments, in which it was calculated from 4 d to 15 and 29 d, respectively (see text)

[c] The percentage of nitrate reduction related to pyrite oxidation was calculated comparing the obtained ratio of nitrate reduction rate to sulfate production rate with the stoichiometry of the overall reaction (eq. 3)

Table 3. Estimated isotopic enrichment factors (εN and εO) obtained in this study and reported in the literature for *in situ* natural denitrification in aquifers and for denitrification in laboratory experiments with sediments from aquifers

εN (‰)	εO (‰)	εN/εO	Reference	Comments
***In situ* studies**				
-22.9	n.d.	2.1	Aravena and Robertson (1998)	septic sands, multilevel wells
-15.9	-8.0	2.1	Bottcher et al. (1990)	gravelly sand, multilevel wells along a groundwater flux line
-13.62	-9.8	1.3	Fukada et al. (2003)	sand and gravel, wells located along a groundwater flux line
-27.6	-18.3	1.5	Mengis et al. (1999)	riparian zone, wells located along a groundwater flux line
-4.7 to -5	n.d.	n.d.	Mariotti et al. (1988)	chalk, wells located along a groundwater flux line
-10	n.d.	n.d.	Spalding and Parrot (1994)	multilevel wells located along a groundwater flux line
-4	n.d.	n.d.	Pauwels et al. (2000)	schist, multilevel wells samples at different time
-7 to -57	n.d.	n.d.	Singleton et al. (2007)	multilevel wells
-13.9	n.d.	n.d.	Smith et al. (1991)	sand and gravel, multilevel wells
-8.38	n.d.	n.d.	Clément et al. (2003)	riparian zone, wells located along a groundwater flux line
-4 to -5.2	n.d.	n.d.	Fustec et al. (1991)	shallow alluvial groundwater, multilevel wells
-17.9	n.d.	n.d.	Tsushima et al. (2002)	sand and gravel, multilevel wells
n.d.	n.d.	1.7	Cey et al. (1999)	multilevel wells
n.d.	n.d.	1.8	Devito et al. (2000)	sand
-4.4 to -15.5	-1.9 to -8.9	0.9 to 2.3	Otero et al. (2009)	carbonate and carbonated-sandstone, confined aquifer (Osona aquifer)
Laboratory studies				
-32.9 to -34.1	n.d.	n.d.	Tsushima et al. (2006)	sediment + groundwater with adjusted nitrate concentration, column experiments
-14.6	n.d.	n.d.	Grischek et al. (1998)	aquifer material + river water, column experiments. Sand, silt and gravel aquifer
-17.8	n.d.	n.d.	Sebilo et al. (2003)	rich muddy river bottom sediments, stirred batch experiments
-27.6	-21.3	1.30	this study, B-2	Osona aquifer sediment + groundwater + pyrite, batch experiment
-25.0	-19.5	1.28	this study, BB-2	Osona aquifer sediment + groundwater + pyrite + *T. denitrificans,* batch experiment

n.d. = not determined

Table 4. Sequence analysis of selected bands from *16S rRNA* gene-based DGGE gel

DGGE band	GenBank accession number	Longitude (pb)	Closest organism in GenBank database (accession number)	% similarity [a]	Phylogenetic group [b]
B1	HM765437	526	*Thiobacillus denitrificans* (AJ243144) [c]	100	*Hydrogenophilaceae (β)*
B7=B20=B21	HM765438/ HM765443	499/526	*Sphingomonas sp*. (AF385529)	100	*Sphingomonadaceae (α)*
B10=B25	HM765439/ HM765444	541/543	*Sediminibacterium sp*. (AB470450)	97	*Chitinophagaceae (B)*
B11=B12=B29	HM765440/ HM765441/ HM765445	547/548/521	Unclassified *β-proteobacteria* (AF351570)	96	*Methylophilaceae (β)*
B19	HM765442	552	Unclassified *γ-proteobacteria* (FJ485034)	95	*Xanthomonadaceae (γ)*
B30=B34	HM765446/ HM765447	490	Unclassified *γ-proteobacteria* (FJ485034)	98	*Xanthomonadaceae (γ)*
B39	HM765448	511	Uncultured *Siderooxidans*	99	*Rhodocyclaceae / Gallionellaceae (β)*
B40	HM765449	487	Uncultured *Methanogenium sp*. (GU247798.1)	99	*Methanomicrobiaceae (E)*

[a] Sequences were aligned against the GenBank database with the BLAST search alignment tool (Altschul et al., 1990) and matched with the closest relative from the GenBank database.
[b] Sequences were matched to phylogenetic groups by using the RDP Naive Bayesian Classifier (Wang et al., 2007); *α*, *β*, *γ*, *B* and *E* represent *α-proteobacteria*, *β-proteobacteria*, *γ-proteobacteria*, *Bacteroidetes* and *Euryarchaeota*, respectively.
[c] The phylogenetic affiliation of the B1 band confirms that the DSMZ 12475 strain used in the combined biostimulated/bioaugmented experiments was *Thiobacillus denitrificans* (100% similarity)